GLL
Geomatics, Landmanagement and Landscape No. 1 • 2026, 71–89

ISSN 2300-1496 https://doi.org/10.15576/GLL/219396

Research paper

Received: 2.02.2026
Accepted: 16.03.2026
Published: 31.03.2026

Improving Landsat 8 and ECOSTRESS surface temperature estimates with in situ surface temperature measurements in Kraków, Poland

Marcin Kucza[1] 0009-0005-2515-3446
Ewa Głowienka[1, ✉] 0000-0001-7326-1592

[1] Department of Photogrammetry, Remote Sensing, and Spatial Engineering, AGH University of Krakow
✉ Corresponding author: eglo@agh.edu.pl

Summary

The study evaluated whether simple site-specific empirical corrections can improve the agreement between Landsat 8 and ECOSTRESS thermal products and ground-based surface temperature logger observations acquired in Kraków, Poland. Three field campaigns conducted in 2023–2024 were paired with Landsat 8 and, when available, ECOSTRESS acquisitions. Two correction approaches, linear regression and additive bias correction, were tested for eight calibration subset configurations representing different urban surface contexts, including paved surfaces, urban parks, heterogeneous urban sites, waterfront locations, spatially dispersed sites, vegetation-covered sites, and a subset defined by low initial mismatch. Performance was assessed using RMSE and the standard deviation of residuals relative to the reference measurements. Both correction approaches reduced disagreement relative to the uncorrected data, but the magnitude of improvement depended strongly on acquisition date, product type, and calibration subset composition. The results show that simple local correction can increase the practical utility of satellite thermal data in a heterogeneous urban setting; however, the findings should be interpreted with caution because contact-based logger measurements are not strictly equivalent to radiometric land surface temperature, and some satellite ground pairs were not fully synchronous.

Keywords

thermal remote sensing • urban surface temperature • Landsat 8 • ECOSTRESS • empirical correction • validation • Google Earth Engine • Kraków

1. Introduction

Satellite thermal remote sensing is widely used to study urban temperature patterns, surface energy exchange, and thermal exposure. In contrast to air temperature networks, satellite observations show the spatial structure of surface heating across entire cities and capture contrasts between densely built-up areas, vegetation, bare ground, and water. This perspective is useful especially in complex urban environments, where thermal conditions change over short distances and are shaped by land cover, morphology, and surface properties [Sobrino et al. 2004, Li et al. 2013, Rasul et al. 2017, Li et al. 2023].

Among the available satellite systems, Landsat remains a core source for urban thermal analysis because it offers a long archive, global coverage, and spatial detail suitable for intra-urban research. Its thermal data have been widely used to map daytime surface temperature and relate it to vegetation, impervious cover, and land use [Malakar et al. 2018, Ermida et al. 2020]. ECOSTRESS adds complementary information by sampling the land surface at varying local times from the International Space Station, which makes it useful for studying the daily thermal cycle and short term thermal contrasts in cities [Fisher et al. 2020, Li et al. 2021, Hurduc et al. 2024, Wei and Sobrino 2024].

At the same time, the use of satellite thermal products in cities raises persistent validation problems. Satellite-derived land surface temperature is not directly equivalent to ground-measured temperature. The satellite sensor records radiometric information integrated over a pixel, while field instruments describe conditions at a point or within a very small area. Agreement therefore depends on emissivity assumptions, atmospheric effects, timing of the acquisition, and spatial representativeness of the validation site [Guillevic et al. 2014, Hu et al. 2014, Yu et al. 2017, Ma et al. 2021, Hulley et al. 2022]. In heterogeneous urban settings, these issues are amplified by mixed pixels and abrupt land cover transitions.

For this reason, many studies distinguish between formal product validation and local empirical adjustment. Simple correction procedures can improve agreement for practical applications, but their performance strongly depends on the reference data used for calibration and on the land cover context of the sampled sites [Li et al. 2021, Meng et al. 2022, Hurduc et al. 2024]. This issue is relevant in Kraków, where earlier work showed clear temperature contrasts related to urban structure, vegetation, and surface cover [Walawender et al. 2014, Głowienka and Micek 2025, Głowienka and Kucza 2025]. Recent comparisons of satellite products and ground observations in Kraków and other cities also indicate that local agreement varies across sensors, dates, and surface types [Głowienka et al. 2025a, Głowienka et al. 2025b].

The present study addresses this problem by evaluating two simple correction approaches, linear regression and additive bias correction, for Landsat 8 and ECOSTRESS observations matched to ground-based surface temperature logger measurements collected in Kraków. The objectives are: to quantify disagreement between the satellite products and field observations; to test whether local correction improves agreement; and to assess how calibration subset composition affects correction stability

under different urban conditions. The study is intended as an operational assessment of empirical correction, not as a full radiometric revalidation of the satellite products.

2. Materials and methods

2.1. Study area

Kraków, a city located in southern Poland on the Vistula River, was selected as the study area because it contains a wide range of urban surface types within a single metropolitan setting, including dense historical fabric, residential districts, transport infrastructure, parks, forests, industrial zones, and water adjacent areas. This diversity makes the city a suitable test bed for evaluating the representativeness of ground observations in relation to moderate resolution thermal satellite products. The spatial distribution of the survey points was designed to capture this heterogeneity and to include both densely built-up and vegetated locations (Fig. 1).

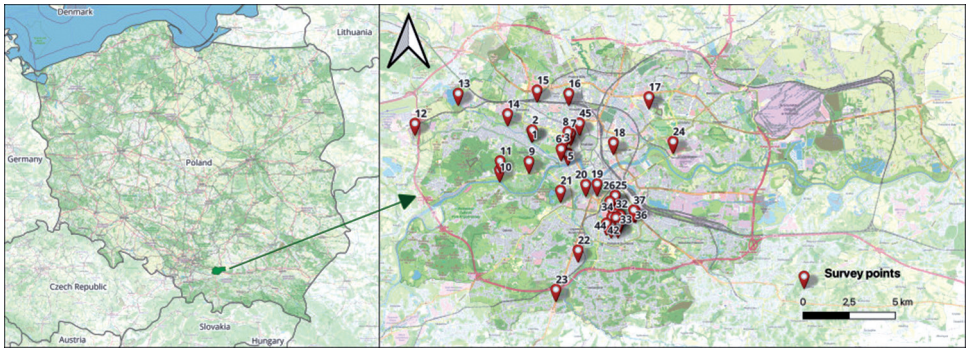

Source: Authors' own study based on OpenStreetMap

Fig. 1. Location of the survey points used in the in situ surface temperature campaign in Kraków, Poland

2.2. In situ surface temperature measurements

Ground observations were collected using Thermochron iButton DS1921G temperature loggers installed at multiple sites representing the main urban surface contexts present in the study area, including parks, paved surfaces, mixed land cover, water adjacent locations, and built-up areas. The sensors recorded contact-based surface temperature and were therefore used as ground-based surface temperature logger measurements rather than as direct radiometric land surface temperature (LST) reference data. This distinction is important because the logger measures temperature at the point of contact with the surface, whereas the satellite product represents pixel scale radiometric temperature. The field campaign was designed to maximize spatial

representativeness and precise geolocation so that the in situ observations could be linked as closely as possible to the corresponding satellite pixels.

Source: Authors' own study

Fig. 2. Examples of representative in situ measurement sites used in the study: a. Park Krakowski (7), b. Water reservoirs Mydlniki (13), c. Bus depot at Wola Duchacka (42), d. Forest next to the Libana quarry (27), e. Vicinity of Bonarka shopping centre (44), f. AGH University of Science and Technology (3)

Satellite acquisitions were selected to correspond as closely as possible to the field campaigns conducted in 2023–2024. Table 1 summarizes the Landsat 8 and ECOSTRESS scenes used in the analysis. For Landsat 8, the source data were Collection 2 Tier 1

Level 1 OLI/TIRS scenes, from which LST was derived in Google Earth Engine. For ECOSTRESS, the source data were the ECO2LSTE Level 2 land surface temperature and emissivity product, which was used directly at product level. The pair for measurement B includes a one day offset between the Landsat 8 and ECOSTRESS acquisitions and should therefore be treated as near synchronous rather than fully simultaneous. This temporal mismatch was retained in the analysis because of data availability, but it is explicitly discussed as a source of uncertainty.

Table 1. Satellite acquisitions used in the analysis. Landsat 8 scenes correspond to Collection 2 Tier 1 Level 1 inputs used for user derived LST retrieval in Google Earth Engine, whereas ECOSTRESS scenes correspond to the ECO2LSTE Level 2 product used directly in the empirical correction workflow. Acquisition time is reported in GMT

Measurement	Mission	Product, processing level (spatial resolution)	Date [yyyy-mm-dd]	GMT time [hh:mm:ss]
A	Landsat 8	C2 T1 L1 OLI/TIRS; LST derived in GEE (100 m)	2023-08-19	09:32:25
	ECOSTRESS	ECO2LSTE (70 m)		09:16:09
B	Landsat 8	C2 T1 L1 OLI/TIRS; LST derived in GEE (100 m)	2024-06-18	09:31:21
	ECOSTRESS	ECO2LSTE (70 m)	2024-06-19	08:16:33
C	Landsat 8	C2 T1 L1 OLI/TIRS; LST derived in GEE (100 m)	2024-07-04	09:31:46

Source: Google Earth Engine

Table 2. Calibration sets used in the empirical correction procedure

Calibration set	Site IDs
Paved surface	24, 17, 15, 12, 22, 20
Urban park	16, 6, 7
Heterogeneous urban	12, 36, 13
Full site network	all sites
Waterfront	20, 19, 13
Spatially dispersed	22, 12, 10, 13, 15, 16, 17, 24
Low initial mismatch	selected individually for each acquisition (2-4 sites)
Vegetated	6, 7, 16, 13

Source: Authors' own study

To test how site selection influences empirical correction performance, the survey points were grouped into several calibration sets representing different urban surface contexts (Table 2). Most sets were defined a priori on the basis of land cover setting or spatial arrangement. The only exception was the 'Low initial mismatch' set, which was defined separately for each acquisition using points with the smallest initial mismatch between ground and satellite temperature. This set was retained for comparison, but its interpretation requires caution because it is partly outcome driven.

- 'Paved surface' – sites located on or adjacent to paved parking surfaces and the surrounding built-up fabric.
- 'Urban park' – sites located in urban parks and other predominantly vegetated recreational areas.
- 'Heterogeneous urban' – sites intentionally selected to represent contrasting urban contexts within a single calibration set.
- 'Full site network' – the full set of available survey points for a given acquisition.
- 'Waterfront' – sites located close to rivers, ponds, or other water bodies.
- 'Spatially dispersed' – sites distributed far apart in space in order to maximize spatial separation.
- 'Low initial mismatch' – sites selected individually for each acquisition on the basis of the smallest initial ground–satellite difference.
- 'Vegetated' – an expanded vegetation dominated set combining park locations and additional green spaces.

The number of sites available for each calibration set varied between acquisitions because some locations contained missing values or could not be matched reliably to the corresponding satellite scene.

2.3. Processing, empirical correction, and accuracy assessment

All analytical steps were carried out in Google Earth Engine (GEE). The Landsat branch of the workflow used Landsat 8 OLI/TIRS Collection 2 Tier 1 Level 1 scenes as the source data. Thus, the Landsat temperatures analysed in this study were not taken from the USGS Level 2 surface temperature product. Instead, land surface temperature was derived by the authors from the Level 1 scene in GEE by means of the NDVI, fractional vegetation, and emissivity procedure summarized in Equations (1)–(4). Within GEE, the Level 1 Landsat scene was transformed to top of atmosphere reflectance and thermal brightness temperature, and these quantities were then used to calculate NDVI, fractional vegetation, emissivity, and the final LST estimate. This is why a separate set of conversion equations is given for Landsat. The approach follows a standard NDVI based emissivity method for Landsat thermal data [Sobrino et al. 2004, EROS Center 2020].

$$NDVI = \frac{\left(NIR - RED\right)}{\left(NIR + RED\right)} \tag{1}$$

where NIR and RED denote the near infrared and red reflectance terms used in Equation (1); for Landsat 8 these correspond to Bands 5 and 4, respectively. Based on the minimum and maximum NDVI values, the fractional vegetation (FV) index was then calculated using Equation (2).

$$FV = \left[\frac{NDVI - NDVI_{\min}}{NDVI_{\max} - NDVI_{\min}} \right]^2 \tag{2}$$

Surface emissivity (EM) was subsequently estimated from the fractional vegetation term:

$$EM = 0.004 \cdot FV + 0.986 \tag{3}$$

where the constant 0.004 represents the emissivity contribution of vegetation and 0.986 represents the emissivity of soil in Equation (3). After emissivity estimation, land surface temperature was calculated using Equation (4) from the Landsat 8 thermal information and used to generate the Landsat temperature maps for the analysed dates.

$$LST = \left(\frac{Tb}{\left(1 + \left(0.00115 \cdot \left(\frac{Tb}{1.438} \right) \right) \cdot \log\left(EM \right) \right)} \right) - 273.15 \tag{4}$$

In Equation (4), Tb denotes the brightness temperature derived from Landsat 8 Band 10. The thermal information has a native spatial resolution of 100 m, although it is delivered on a finer grid in the standard Landsat product. For that reason, the interpretation of the Landsat results in this study is tied to the thermal support of the TIRS measurement rather than to the nominal grid size alone.

In contrast, the ECOSTRESS branch of the analysis used the ECO2LSTE product, which is a Level 2 land surface temperature and emissivity dataset. This product already provides atmospherically corrected LST and emissivity derived from five thermal infrared bands by means of a temperature and emissivity separation algorithm. Therefore, no additional temperature conversion equivalent to the Landsat procedure was applied to ECOSTRESS. ECOSTRESS temperatures were extracted directly from the Level 2 LST layer and then entered into the same empirical correction framework as the Landsat results [Fisher et al. 2020, Hook and Hulley 2019].

Figure 3 provides an overview of the data integration workflow, the Landsat Level 1 to LST processing sequence, and the direct use of ECOSTRESS Level 2 temperature data.

Empirical correction was applied separately for each acquisition, product, and calibration subset after Landsat Level 1 scenes had been transformed to LST and ECOSTRESS Level 2 temperatures had been extracted from the product layer. Two correction models were evaluated. In the linear regression approach, corrected temperature was computed as:

$$T_{corr} = a \cdot T_{sat} + b \quad (5)$$

where T_{sat} is the satellite-derived temperature and a and b are regression coefficients estimated from the calibration set.

In the additive bias correction approach, corrected temperature was computed as:

$$T_{corr} = T_{sat} + \text{mean}\,(T_{ref} - T_{sat}) \quad (6)$$

where T_{ref} is the ground-based surface temperature logger measurement.

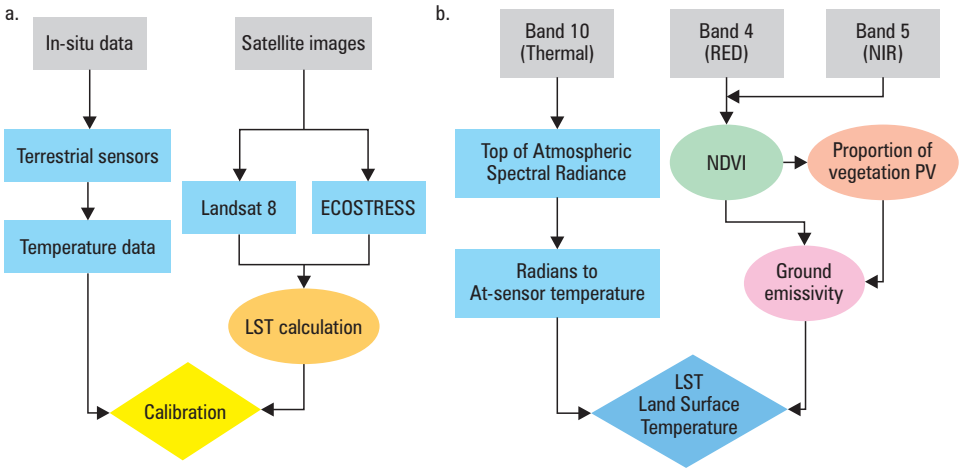

Source: Authors' own study

Fig. 3. Overview of the analytical workflow: a. integration of in situ observations with satellite-derived temperature data; b. Landsat 8 Collection 2 Tier 1 Level 1 processing used for LST retrieval in Google Earth Engine. ECOSTRESS temperatures were extracted directly from the ECO2LSTE Level 2 product and were not recalculated from raw thermal data

Model performance was assessed using RMSE and the standard deviation of residuals relative to the reference measurements. Because the reference data are contact based and the satellite temperatures represent pixel scale radiometric values, the analysis should be interpreted as an empirical agreement assessment rather than as absolute validation of LST accuracy. Additional uncertainty arises from temporal mismatch between acquisitions and from the point to pixel representativeness problem in heterogeneous urban surfaces.

3. Results

The empirical correction procedure reduced disagreement between the satellite-derived temperature values and the ground-based surface temperature logger observations, but the magnitude and stability of the improvement depended on the acquisition date, the

satellite product, and the composition of the calibration set. Across both correction approaches, the results showed that calibration set composition strongly influenced error statistics, which indicates that local surface context matters as much as the choice of the correction formula itself.

3.1. Linear regression

Linear regression correction improved agreement for several calibration sets, although the response varied across acquisitions and products (Fig. 4). For measurement A, the reference standard deviation was approximately 7–8°C, whereas for measurement B it was approximately 4–4.5°C. For measurement C (Landsat 8 only), the reference standard deviation was 5.78°C. The 'Paved surface' set frequently produced low RMSE values, ranging from 2.22°C in measurement C to 4.63°C in measurement B. The 'Urban park' and 'Vegetated' sets were generally associated with lower standard deviation of residuals, indicating reduced within-set dispersion. The 'Low initial mismatch' set usually yielded the lowest or one of the lowest RMSE values. However, because this set was selected using the smallest initial mismatch between ground and satellite data, its performance should be interpreted as an optimistic scenario rather than as independent evidence of predictive accuracy. Overall, the linear regression results suggest that the method is most useful when the calibration set represents thermally coherent surface conditions.

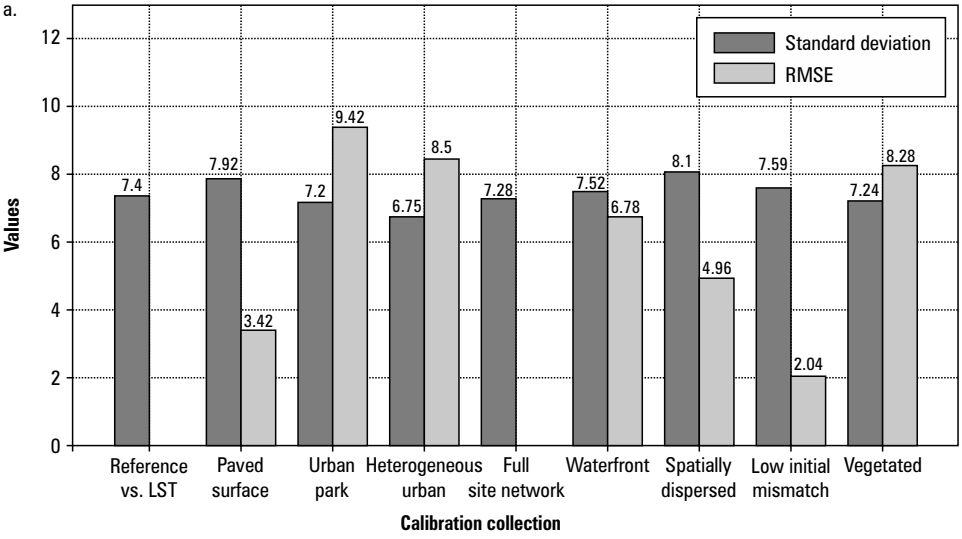

Source: Authors' own study

Fig. 4. Standard deviation of residuals and RMSE for the different calibration sets after linear regression correction: a. Landsat 8, August 2023 (measurement A). b. ECOSTRESS, August 2023 (measurement A). c. Landsat 8, June 2024 (measurement B). d. ECOSTRESS, June 2024 (measurement B). e. Landsat 8, July 2024 (measurement C)

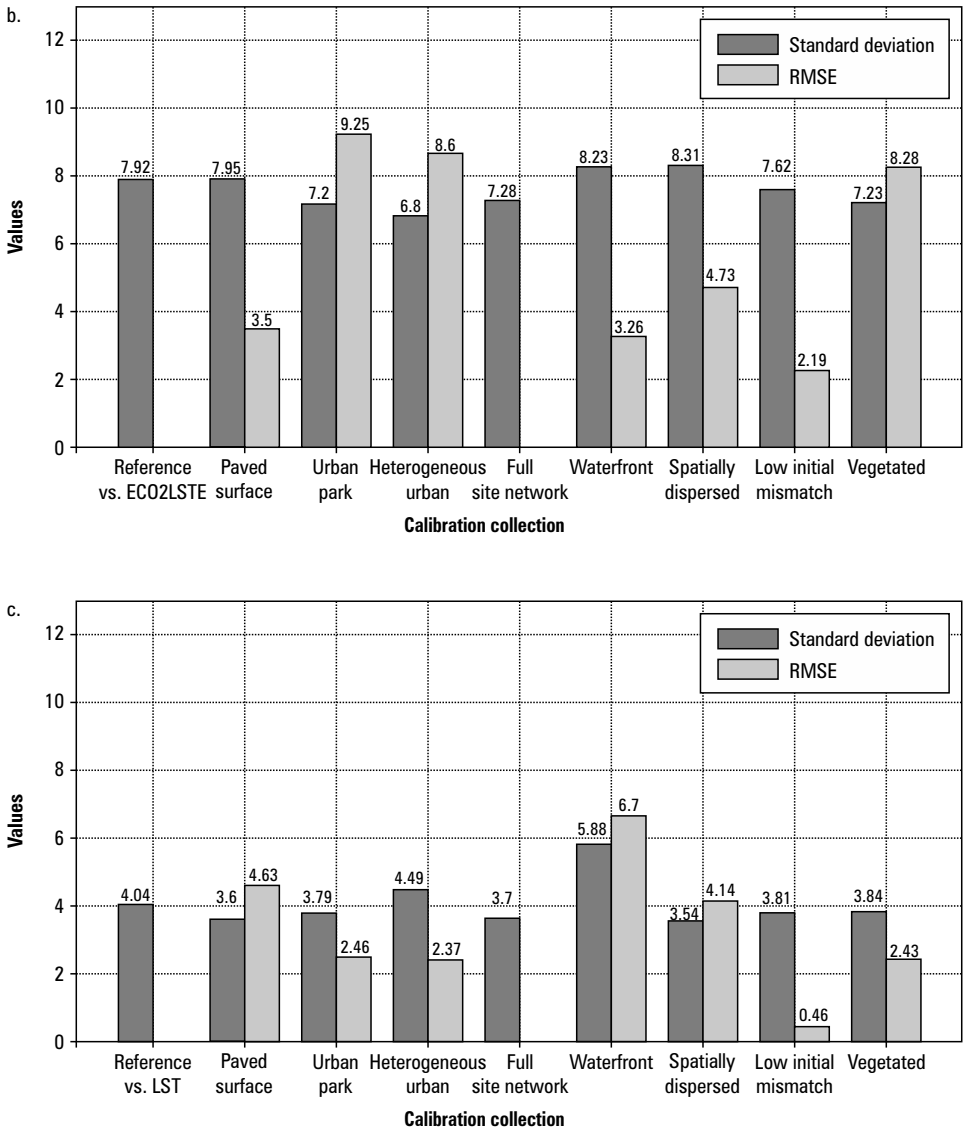
b.
Standard deviation
RMSE
Values
0
2
4
6
8
10
12
7.92
7.95
3.5
7.2
9.25
6.8
8.6
7.28
8.23
3.26
8.31
4.73
7.62
2.19
7.23
8.28
Reference vs. ECO2LSTE
Paved surface
Urban park
Heterogeneous urban
Full site network
Waterfront
Spatially dispersed
Low initial mismatch
Vegetated
Calibration collection
c.
Standard deviation
RMSE
Values
0
2
4
6
8
10
12
4.04
3.6
4.63
3.79
2.46
4.49
2.37
3.7
5.88
6.7
3.54
4.14
3.81
0.46
3.84
2.43
Reference vs. LST
Paved surface
Urban park
Heterogeneous urban
Full site network
Waterfront
Spatially dispersed
Low initial mismatch
Vegetated
Calibration collection

Fig. 4. cont.

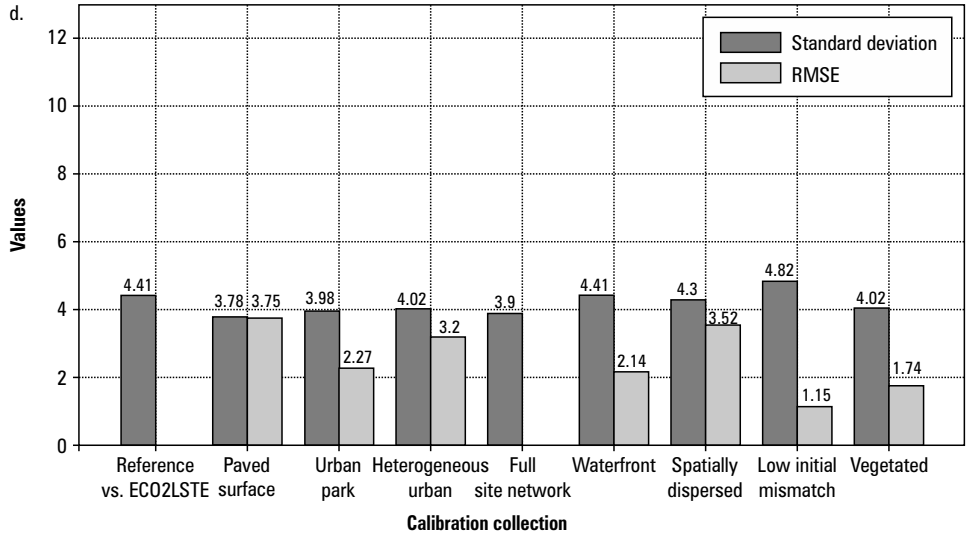
d.
Standard deviation
RMSE
Values
0
2
4
6
8
10
12
4.41
3.78
3.75
3.98
2.27
4.02
3.2
3.9
4.41
2.14
4.3
3.52
4.82
1.15
4.02
1.74
Reference vs. ECO2LSTE
Paved surface
Urban park
Heterogeneous urban
Full site network
Waterfront
Spatially dispersed
Low initial mismatch
Vegetated
Calibration collection

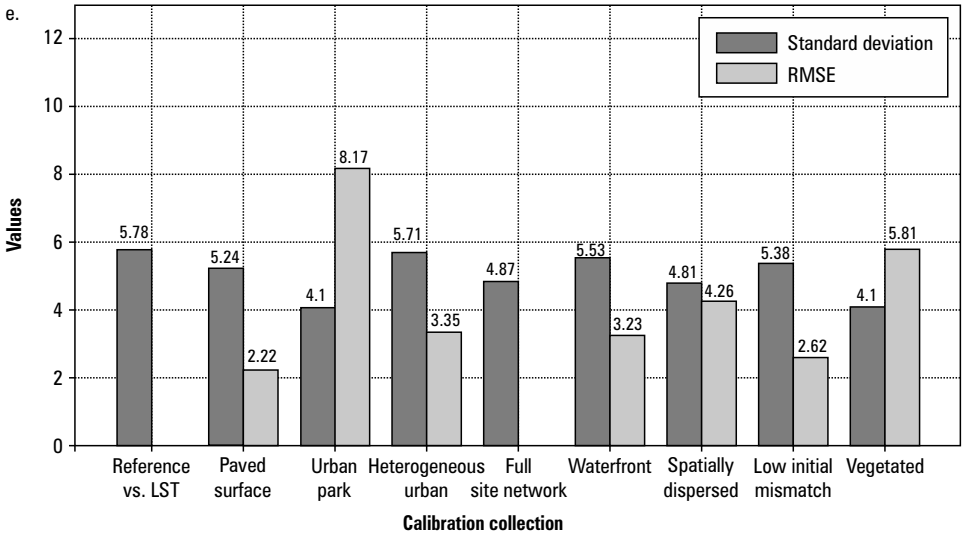
e.
Standard deviation
RMSE
Values
0
2
4
6
8
10
12
5.78
5.24
2.22
4.1
8.17
5.71
3.35
4.87
5.53
3.23
4.81
4.26
5.38
2.62
4.1
5.81
Reference vs. LST
Paved surface
Urban park
Heterogeneous urban
Full site network
Waterfront
Spatially dispersed
Low initial mismatch
Vegetated
Calibration collection

Fig. 4. cont.

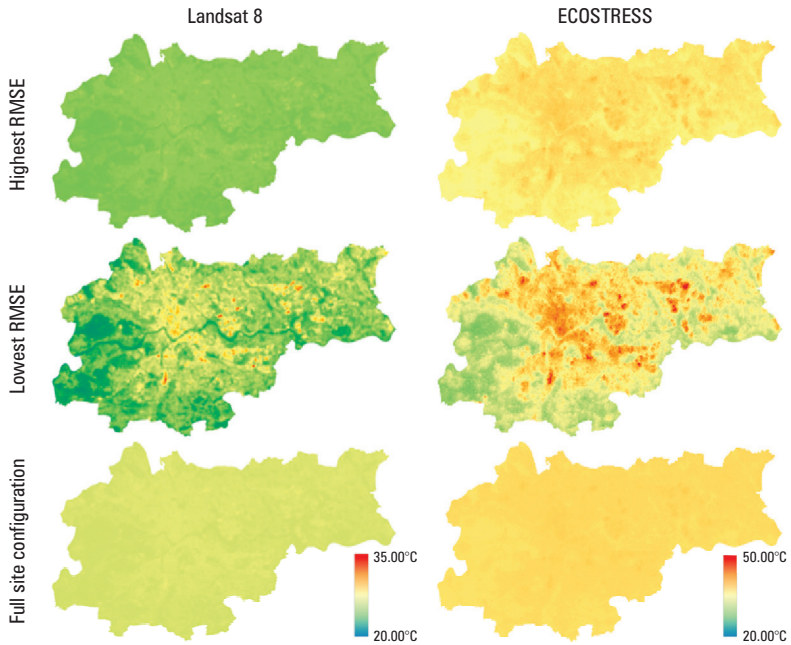

Source: Authors' own study

Fig. 5. Comparison of Landsat 8 and ECOSTRESS temperature maps after linear regression correction for the August 2023 acquisition (measurement A). Columns show Landsat 8 and ECOSTRESS, respectively. Rows show, from top to bottom, the highest RMSE case (urban park subset), the lowest RMSE case (low initial mismatch subset), and the full site network

3.2. Bias correction

Additive bias correction also reduced systematic disagreement, although its performance was less consistent across calibration sets than that of linear regression (Fig. 6). The 'Waterfront' set often retained high RMSE values and reached approximately 12°C in the August 2023 ECOSTRESS case. The 'Low initial mismatch' set again produced the lowest RMSE values, but this reflects the outcome dependent way in which the set was defined. The 'Urban park' and 'Vegetated' sets showed similar central tendency, with differences generally within 0.3°C, except for July 2024 when the difference for 'Urban park' increased to about 2°C. The 'Spatially dispersed' set produced one of the lowest standard deviations in July 2024 (4.15°C) despite a relatively high RMSE of 7.75°C, indicating low internal dispersion but persistent bias. Overall, bias correction proved useful for removing systematic offsets, whereas linear regression more clearly captured variation among the calibration set configurations.

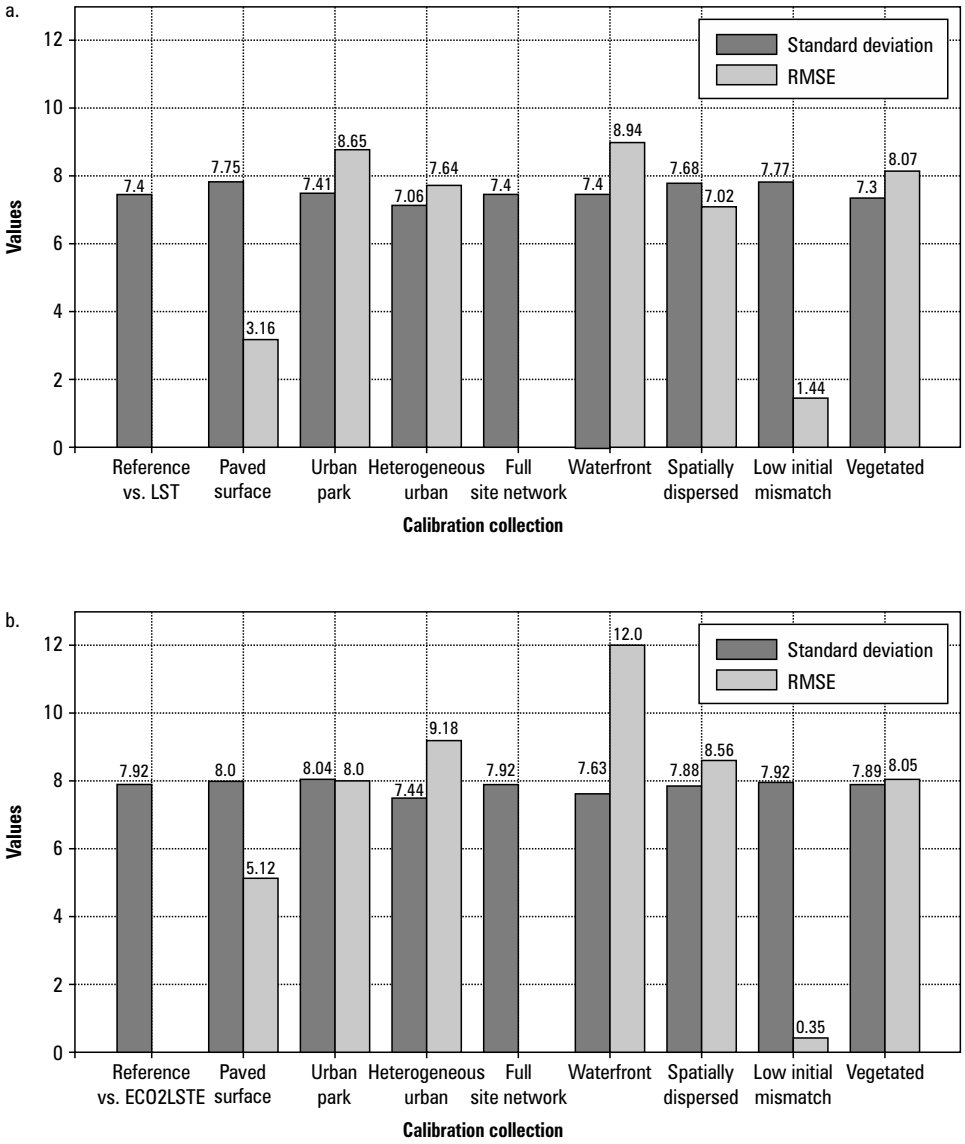

Source: Authors' own study

Fig. 6. Standard deviation of residuals and RMSE for the different calibration sets after additive bias correction: a. Landsat 8, August 2023 (measurement A). b. ECOSTRESS, August 2023 (measurement A). c. Landsat 8, June 2024 (measurement B). d. ECOSTRESS, June 2024 (measurement B). e. Landsat 8, July 2024 (measurement C)

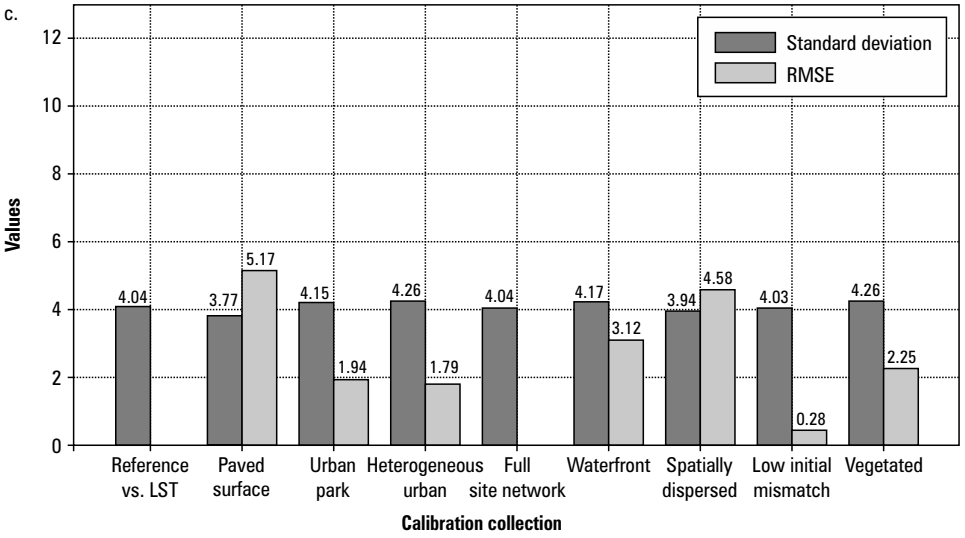
c.
Standard deviation
RMSE
Values
0
2
4
6
8
10
12
4.04
3.77
5.17
4.15
1.94
4.26
1.79
4.04
4.17
3.12
3.94
4.58
4.03
0.28
4.26
2.25
Reference vs. LST
Paved surface
Urban park
Heterogeneous urban
Full site network
Waterfront
Spatially dispersed
Low initial mismatch
Vegetated
Calibration collection

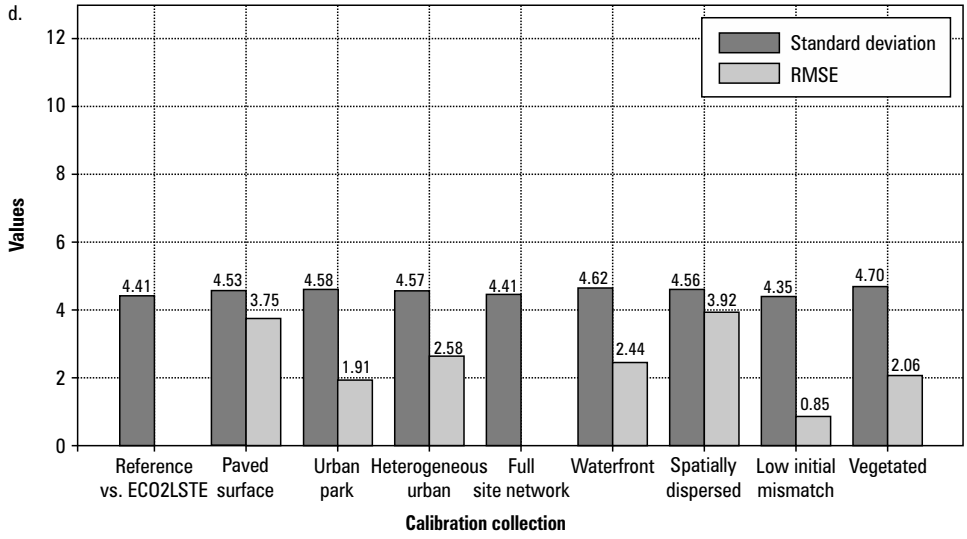
d.
Standard deviation
RMSE
Values
0
2
4
6
8
10
12
4.41
4.53
3.75
4.58
1.91
4.57
2.58
4.41
4.62
2.44
4.56
3.92
4.35
0.85
4.70
2.06
Reference vs. ECO2LSTE
Paved surface
Urban park
Heterogeneous urban
Full site network
Waterfront
Spatially dispersed
Low initial mismatch
Vegetated
Calibration collection

Fig. 6. cont.

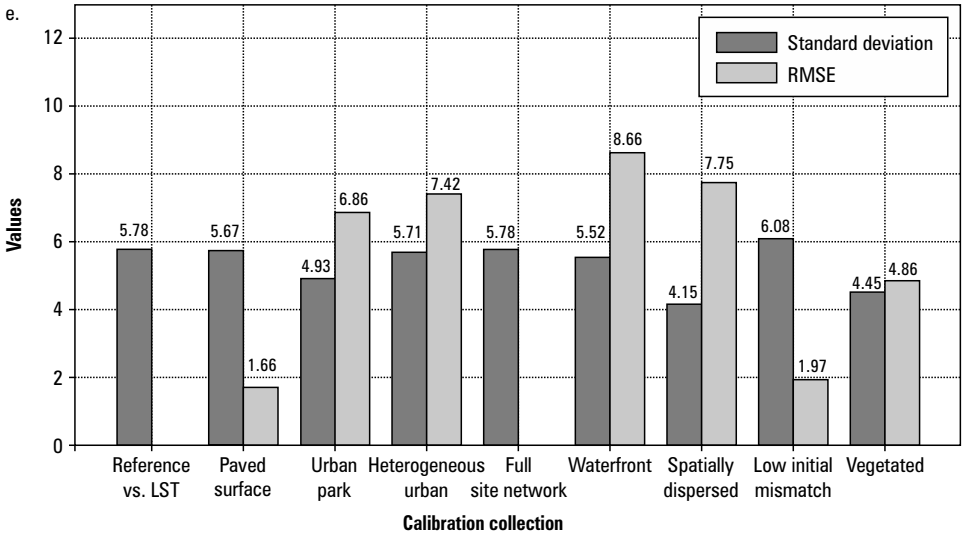

Fig. 6. cont.

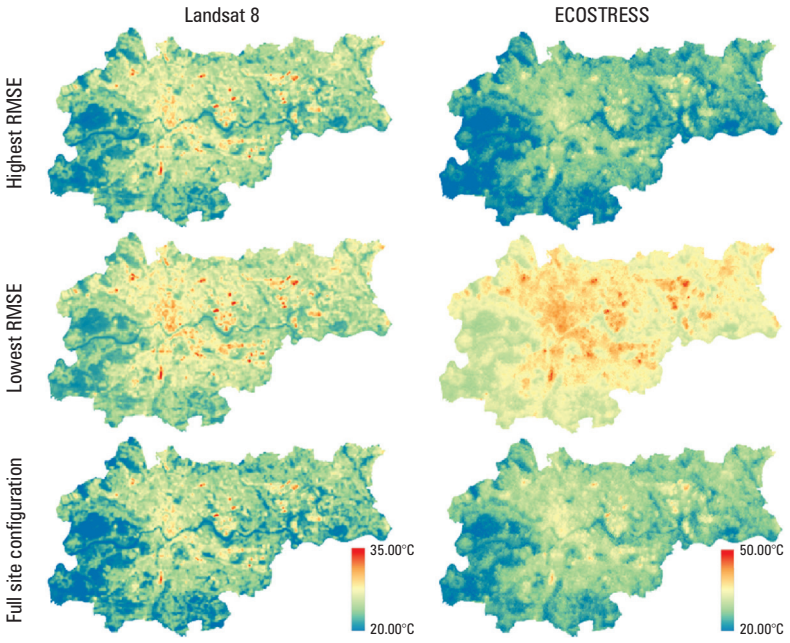

Source: Authors' own study

Fig. 7. Illustrative comparison of Landsat 8 and ECOSTRESS temperature maps after additive bias correction for the August 2023 acquisition (measurement A). Panels correspond to the calibration set configurations with the largest error, the smallest error, and the full site configuration

4. Discussion

The results show that simple local correction can improve agreement between Landsat 8, ECOSTRESS, and ground-based surface temperature logger measurements, but the effect is not uniform across products, dates, and calibration subsets. This supports a cautious view of empirical correction. Its value depends not only on the correction formula, but also on the quality and representativeness of the reference data. Similar conclusions have been reported in the broader validation literature, where residual disagreement is shaped by surface heterogeneity, sampling design, and spatial representativeness as much as by sensor properties alone [Guillevic et al. 2014, Yu et al. 2017, Ma et al. 2021, Hulley et al. 2022, Głowienka et al. 2025a].

One of the clearest outcomes of this study is the role of calibration subset composition. Subsets linked to more thermally coherent urban contexts usually produced more stable residual patterns than groups with stronger internal heterogeneity or more complex local conditions. This is consistent with studies showing that the apparent quality of a thermal product depends strongly on the representativeness of the reference site and on the point to pixel relation used in validation [Yu et al. 2017, Ma et al. 2021]. The strong performance of the low initial mismatch subset should therefore be treated with caution, because this subset was defined by its initial agreement with the satellite temperature and cannot be read as independent evidence of predictive skill.

The comparison between Landsat 8 and ECOSTRESS also fits the existing literature. Landsat remains a stable baseline for medium resolution urban thermal mapping, while ECOSTRESS provides valuable information on acquisition timing and the daily thermal cycle [Malakar et al. 2018, Ermida et al. 2020, Fisher et al. 2020, Hurduc et al. 2024]. In the present data, ECOSTRESS added useful observations, but it did not consistently produce lower residual disagreement after correction. The importance of land cover context seen here is also consistent with earlier work from Kraków and other Central European cities, where temperature patterns were linked to urban structure, vegetation, and the cooling role of green areas [Walawender et al. 2014, Cao et al. 2010, Blachowski and Hajnrych 2021, Głowienka and Micek 2025, Głowienka and Kucza 2025].

The results should also be interpreted in light of several methodological limits. The field observations were obtained with contact sensors, so they are not equivalent to radiometric land surface temperature. The comparison is also affected by point to pixel mismatch, because the logger describes local conditions while the satellite product represents a much larger support area. In addition, temporal correspondence between field and satellite data was imperfect for some campaigns. These are well known constraints in thermal validation studies and they limit the strength of any claim about absolute product accuracy [Hu et al. 2014, Guillevic et al. 2014, Yu et al. 2017, Hulley et al. 2022].

From an applied perspective, the results suggest that simple empirical correction can support local urban climate studies when the aim is comparative mapping or practical adjustment of satellite temperature data within one city. Future work should therefore focus on independent validation data, clearer point to pixel sampling rules, and a broader set of error metrics. The inclusion of radiometric reference measurements

would also make it easier to separate product error from representativeness error and improve the transferability of the workflow to other cities, seasons, and surface contexts [Głowienka et al. 2025a, Głowienka et al. 2025b, Wei and Sobrino 2024].

5. Conclusions

The study demonstrates that simple empirical correction can improve the agreement between Landsat 8 and ECOSTRESS temperature products and ground-based surface temperature logger observations in a heterogeneous urban setting. Both linear regression and additive bias correction reduced disagreement relative to the uncorrected data, but their effectiveness depended strongly on the calibration subset composition, acquisition date, and sensor type. The results therefore support the use of site-specific correction as a practical adjustment procedure rather than as a substitute for rigorous product validation. Future research should prioritise independent validation, stricter satellite-ground synchronisation, explicit treatment of pixel representativeness, and, where possible, the use of radiometric surface temperature reference measurements.

References

Blachowski J., Hajnrych M. 2021. Assessing the Cooling Effect of Four Urban Parks of Different Sizes in a Temperate Continental Climate Zone: Wroclaw (Poland). Forests 12, 1136. https://doi.org/10.3390/f12081136

Cao X., Onishi A., Chen J., Imura H. 2010. Quantifying the cool island intensity of urban parks using ASTER and IKONOS data. Landsc. Urban Plan., 96, 224–231. https://doi.org/10.1016/j.landurbplan.2010.03.008

Earth Resources Observation and Science (EROS) Center. 2020. Landsat 8-9 Operational Land Imager / Thermal Infrared Sensor Level-1, Collection 2 [dataset]. U.S. Geological Survey. https://doi.org/10.5066/P975CC9B

Ermida S.L., Soares P., Mantas V., Göttsche F.-M., Trigo I.F. 2020. Google Earth Engine Open-Source Code for Land Surface Temperature Estimation from the Landsat Series. Remote Sens., 12, 1471. https://doi.org/10.3390/rs12091471

Fisher J.B., Lee B., Purdy A.J., Halverson G.H., Dohlen M.B., Cawse-Nicholson K. et al. 2020. ECOSTRESS: NASA's Next Generation Mission to Measure Evapotranspiration from the International Space Station. Water Resour. Res., 56, e2019WR026058. https://doi.org/10.1029/2019WR026058

Głowienka E., Kucza M. 2025. Persistent Urban Park Cooling Effects in Krakow: A Satellite-Based Analysis of Land Surface Temperature Patterns (1990–2018). Remote Sens., 17, 3608. https://doi.org/10.3390/rs17213608

Głowienka E., Malinverni E.S., Sanità M., Michałowska K., Kucza M. 2025a. Harmonizing satellite thermal data with ground-based observations for climate long-term monitoring. Int. Arch. Photogramm. Remote Sens. Spatial Inf. Sci., XLVIII-M-7-2025, 127–132. https://doi.org/10.5194/isprs-archives-XLVIII-M-7-2025-127-2025

Głowienka E., Malinverni E.S., Kucza M., Michałowska K., Sanità M. 2025b. Satellite and ground-based data to monitor urban heat islands. Cases of study: Polish and Italian cities. Int. Arch. Photogramm. Remote Sens. Spatial Inf. Sci., XLVIII-G-2025, 521–527. https://doi.org/10.5194/isprs-archives-XLVIII-G-2025-521-2025

Głowienka E., Micek Z. 2025. Multitemporal assessment of Krakow's urban microclimate (2002–2023) using satellite-derived land surface temperature, NDVI, and NDBI. Geomat. Landmanag. Landsc., 3, 215–233. https://doi.org/10.15576/GLL/211223

Guillevic P.C., Biard J.C., Hulley G.C., Privette J.L., Hook S.J., Olioso A., Göttsche F.M., Radocinski R., Roman M.O., Yu Y., Csiszar I. 2014. Validation of Land Surface Temperature products derived from the Visible Infrared Imaging Radiometer Suite (VIIRS) using ground-based and heritage satellite measurements. Remote Sens. Environ., 154, 19–37. https://doi.org/10.1016/j.rse.2014.08.013

Hu L., Brunsell N.A., Monaghan A.J., Barlage M., Wilhelmi O.V. 2014. How can we use MODIS land surface temperature to validate long-term urban model simulations? J. Geophys. Res. Atmos., 119, 3185–3201. https://doi.org/10.1002/2013JD021101

Hook S., Hulley G. 2019. ECOSTRESS Land Surface Temperature and Emissivity Daily L2 Global 70 m V001 [dataset]. NASA Land Processes Distributed Active Archive Center. https://doi.org/10.5067/ECOSTRESS/ECO2LSTE.001

Hulley G.C., Göttsche F.-M., Rivera G., Hook S.J., Freepartner R., Cawse-Nicholson K. et al. 2022. Validation and Quality Assessment of the ECOSTRESS Level-2 Land Surface Temperature and Emissivity Product. IEEE Trans. Geosci. Remote Sens., 60, 1–23. https://doi.org/10.1109/TGRS.2021.3079879

Hurduc A., Ermida S.L., DaCamara C.C. 2024. On the Suitability of Different Satellite Land Surface Temperature Products to Study Surface Urban Heat Islands. Remote Sens., 16, 3765. https://doi.org/10.3390/rs16203765

Li K., Guan K., Jiang C., Wang S., Peng B., Cai Y. 2021. Evaluation of Four New Land Surface Temperature (LST) Products in the U.S. Corn Belt: ECOSTRESS, GOES-R, Landsat, and Sentinel-3. IEEE J. Sel. Top. Appl. Earth Obs. Remote Sens., 14, 9931–9945. https://doi.org/10.1109/JSTARS.2021.3114613

Li Z.-L., Tang B.-H., Wu H., Ren H., Yan G., Wan Z., Trigo I.F., Sobrino J.A. 2013. Satellite-derived land surface temperature: Current status and perspectives. Remote Sens. Environ., 131, 14–37. https://doi.org/10.1016/j.rse.2012.12.008

Li Z.-L., Wu H., Duan S.-B., Zhao W., Ren H., Liu X. et al. 2023. Satellite Remote Sensing of Global Land Surface Temperature: Definition, Methods, Products, and Applications. Rev. Geophys., 61, e2022RG000777. https://doi.org/10.1029/2022RG000777

Ma J., Zhou J., Liu S., Göttsche F.-M., Zhang X., Wang S., Li M. 2021. Continuous evaluation of the spatial representativeness of land surface temperature validation sites. Remote Sens. Environ., 265, 112669. https://doi.org/10.1016/j.rse.2021.112669

Malakar N.K., Hulley G.C., Hook S.J., Laraby K., Cook M., Schott J.R. 2018. An Operational Land Surface Temperature Product for Landsat Thermal Data: Methodology and Validation. IEEE Trans. Geosci. Remote Sens., 56, 5717–5735. https://doi.org/10.1109/TGRS.2018.2824828

Meng X., Cheng J., Zhao S., Guo Y. 2022. Validation of the ECOSTRESS Land Surface Temperature Product Using Ground Measurements. IEEE Geosci. Remote Sens. Lett., 19, 3005305. https://doi.org/10.1109/LGRS.2021.3123816

Rasul A., Balzter H., Smith C., Remedios J., Adamu B., Sobrino J.A., Srivanit M., Weng Q. 2017. A Review on Remote Sensing of Urban Heat and Cool Islands. Land, 6, 38. https://doi.org/10.3390/land6020038

Sobrino J.A., Jiménez-Muñoz J.C., Paolini L. 2004. Land surface temperature retrieval from LANDSAT TM 5. Remote Sens. Environ., 90, 434–440. https://doi.org/10.1016/j.rse.2004.02.003

Walawender J.P., Szymanowski M., Hajto M.J., Bokwa A. 2014. Land Surface Temperature Patterns in the Urban Agglomeration of Krakow (Poland) Derived from Landsat-7/ETM+ Data. Pure Appl. Geophys., 171, 913–940. https://doi.org/10.1007/s00024-013-0685-7

Wei L., Sobrino J.A. 2024. Surface urban heat island analysis based on local climate zones using ECOSTRESS and Landsat data: A case study of Valencia city (Spain). Int. J. Appl. Earth Obs. Geoinf., 130, 103875. https://doi.org/10.1016/j.jag.2024.103875

Yu W., Ma M., Li Z., Tan J., Wu A. 2017. New Scheme for Validating Remote-Sensing Land Surface Temperature Products with Station Observations. Remote Sens., 9, 1210. https://doi.org/10.3390/rs9121210